NANO LETTERS

Letter

pubs.acs.org/NanoLett

Boosting Solar Cell Photovoltage via Nanophotonic Engineering

Y. Cui,[†] D. van Dam,[*,†] S. A. Mann,[‡] N. J. J. van Hoof,[†] P. J. van Veldhoven,[†] E. C. Garnett,[‡] E. P. A. M. Bakkers,[†,§] and J. E. M. Haverkort[*,†]

[†]Applied Physics, Eindhoven University of Technology, P.O. Box 513, 5600 MB Eindhoven, The Netherlands

[‡]Center for Nanophotonics, FOM Institute AMOLF, 1098 XG Amsterdam, The Netherlands

[§]Kavli Institute of Nanoscience, Delft University of Technology, 2600 GA Delft, The Netherlands

Supporting Information

ABSTRACT: Approaching the theoretically limiting open circuit voltage (V_{oc}) of solar cells is crucial to optimize their photovoltaic performance. Here, we demonstrate experimentally that nanostructured layers can achieve a fundamentally larger Fermi level splitting, and thus a larger V_{oc}, than planar layers. By etching tapered nanowires from planar indium phosphide (InP), we directly compare planar and nanophotonic geometries with the exact same material quality. We show that the external radiative efficiency of the nanostructured layer at 1 sun is increased by a factor 14 compared to the planar layer, leading to a 70 mV enhancement in V_{oc}. The higher voltage arises from both the enhanced outcoupling of photons, which promotes radiative recombination, and the lower active material volume, which reduces bulk recombination. These effects are generic and promise to enhance the efficiency of current record planar solar cells made from other materials as well.

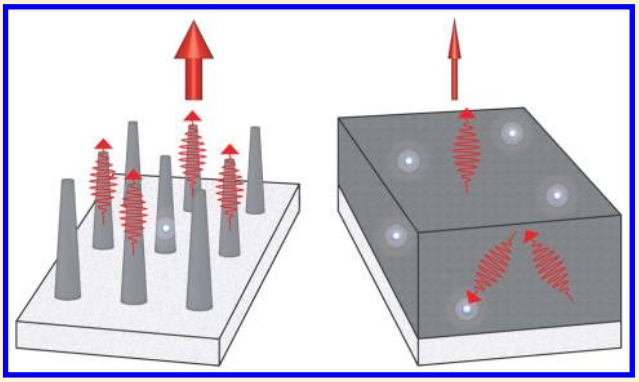

KEYWORDS: *Nanophotonics, photovoltaics, nanowires, photovoltage, open circuit voltage*

To maximize the conversion efficiency of sunlight into electricity, a photovoltaic device needs to simultaneously achieve optimal photocurrent and voltage. Nanophotonic engineering has been employed to enhance the photocurrent of solar cells by reducing reflection and increasing solar light absorption via light trapping,[1−7] and values close to full absorption have already been achieved.[8] Therefore, to bring the photovoltaic conversion efficiency closer to the theoretical limit as determined by Shockley and Queisser,[9] the open circuit voltage (V_{oc}) needs to be further improved.[10−13] The V_{oc} is generally expressed as a function of photocurrent density J_{sc} and dark current density J_0 as $V_{oc} \approx \frac{k_B T}{q} \ln \frac{J_{sc}}{J_0}$, in which k_B, T, and q are the Boltzmann constant, solar cell temperature, and electron charge, respectively.[14]

The dark (saturation) current density is proportional to the recombination rate and can be separated into a radiative part and a nonradiative part. Maximizing the voltage requires minimizing recombination, but even a perfect solar cell must undergo radiative recombination to remain in thermal equilibrium with its surroundings. As such, radiative recombination is not a loss but a thermodynamic necessity, and optimizing external light emission therefore improves solar cell performance.[15] However, nonradiative recombination caused by bulk defect and surface recombination, constitutes a loss that can be eliminated. Therefore, improving the V_{oc} requires increasing the ratio of external radiative to total recombination rates, which is equivalent to increasing the external radiative efficiency (η_{ext}). This fact implies that optimization of a solar cell's power output requires not only maximizing the internal radiative efficiency (η_{int}), which gives the fraction of internal recombination events that is radiative, but also optimizing the average escape probability of an internally emitted photon ($\overline{P_{esc}}$). This counterintuitive phenomenon is explained in more detail elsewhere[15−17] and in the Supporting Information. Bulk (Shockley−Read−Hall) nonradiative recombination in a solar cell is proportional to the amount of active material, which means that η_{int} can be improved by reducing the amount of material[18] if surface recombination plays a minor role. Additionally, efficient outcoupling of internally emitted photons is essential because it prevents eventual nonradiative recombination due to photon reabsorption.[15] Therefore, reducing the amount of absorber material and enhancing the $\overline{P_{esc}}$ of emitted photons can improve the V_{oc}. This becomes directly apparent from the equation for the V_{oc} (valid for $\eta_{int} < \sim 0.1$):

$$V_{oc} = V_{oc}^{rad} - \frac{k_B T}{q} |\ln \eta_{int} \overline{P_{esc}}| \quad (1)$$

Received: July 18, 2016
Revised: August 29, 2016
Published: September 8, 2016

DOI: 10.1021/acs.nanolett.6b02971
Nano Lett. 2016, 16, 6467−6471

where V_{oc}^{rad} is the V_{oc} in the radiative limit (in the absence of nonradiative recombination; see the derivation in the Supporting Information). This shows that improvements in η_{int} and $\overline{P_{esc}}$ are equally important for increasing the V_{oc}. For improving η_{int} by reducing material volume, we need to make sure to simultaneously maintain maximum absorption of sunlight. This can be achieved using the antenna effect of nanostructures, which allows them to absorb light from a larger area than their projected geometrical area.[3,13,19] For minimizing losses due to the $\overline{P_{esc}}$ term, enhanced outcoupling of internally generated photons can be achieved in tapered nanowires by utilizing adiabatic expansion of the optical mode confined in the nanowire into free space.[20] The two described mechanisms, applied to tapered nanowires, are schematically displayed in Figure 1a. Figure 1b shows the effects on the V_{oc}, including a

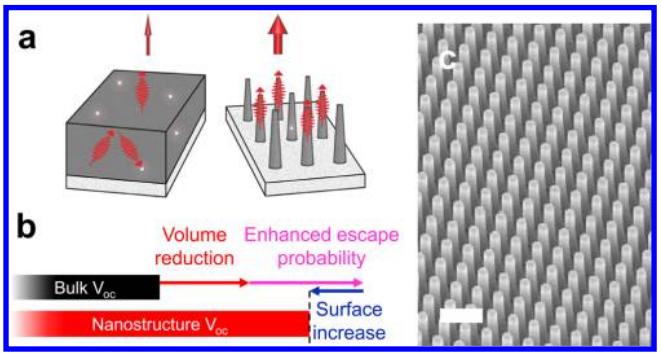

Figure 1. Effect of nanowire geometry on V_{oc}. (a) A planar InP sample is compared to a piece of the same material in which a nanowire structure is defined by etching; the emission outcoupling is enhanced, and the number of bulk defect is reduced. (b) Schematic of the effects of the nanostructuring on the V_{oc}. Because of reduced bulk recombination and enhanced outcoupling, the emission intensity (red upward arrow) is enhanced, indicating a higher V_{oc}. (c) Scanning electron micrograph of the etched nanowire array, imaged at a 30 degree tilt. The scale bar represents 1 μm.

possible reduction due to the increased surface area. A high V_{oc} in a nanostructured solar cell has been reported recently,[21] but it could not be directly compared to the planar geometry because of the nanowire's crystal structure and the growth mechanism, which is different from that of planar layers. Here, we demonstrate that nanostructuring enhances the V_{oc} of the identical material in planar morphology due to the two mechanisms described above.

To investigate the effect of nanostructuring on the V_{oc}, we compare planar indium phosphide (InP) material to a piece from the same sample in which we have defined nanostructures by top-down lithographic techniques. The planar and nanostructured samples thus consist of identical material from the same growth run, which allows us to isolate the effect of nanostructuring on the V_{oc}. We use an intrinsic epitaxial InP layer of 1600 nm grown by metal−organic vapor-phase epitaxy (MOVPE) on top of an InP wafer. We chose InP because it has a direct band gap with the ideal energy for photovoltaic devices (E_g = 1.34 eV) and a low surface recombination velocity.[22] The nanostructured sample (a periodic array of conically shaped nanowires) is fabricated by selectively dry etching the thin film through a chromium mask patterned by nanoimprint lithography, followed by digital etching to remove surface defects (more information is given in the Methods section). The result is shown in a scanning electron micrograph in Figure 1c. The period of our square array is 513 nm, where the 1.6 μm long tapered wires have a base diameter of 350 nm and a top diameter of 150 nm. The conical shape is chosen because of its very high absorptance,[6,19,23] which, for InP, can be over 98% in the full wavelength range of between 400 and 900 nm.[19]

To compare the V_{oc} with and without nanostructuring, we use the fact that the photoluminescence (PL) emission intensity in a semiconductor is directly related to the splitting of its quasi-Fermi levels[24−27] (see the Supporting Information). We can therefore use calibrated PL measurements as a contactless probe for the V_{oc}. PL emission spectra of InP with and without nanostructuring are shown in Figure 2a

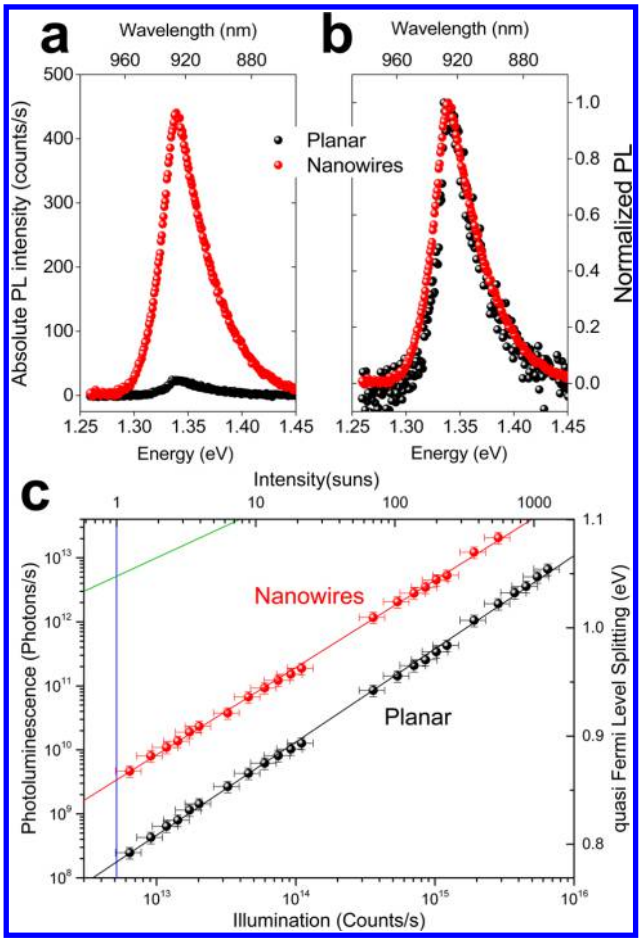

Figure 2. Determination of quasi-Fermi level splitting by photoluminescence. Photoluminescence spectra of (a) planar layer (black) and nanowire layer (red). (b) Same as (a), but the spectra are normalized to their respective maxima to allow for comparison of the shapes. (c) Power-dependent PL for planar (black) and nanostructured (red) InP films, corrected for absorption at the PL wavelength. The illumination intensity is converted into suns (top axis), and the PL intensity is expressed as Fermi level splitting (right axis). The blue line corresponds to 1 sun, and the green line is the ideal curve for a sample with external radiative efficiency equal to 1. The red and black curves are linear fits through the data.

(absolute counts) and 2b (normalized counts), measured at room temperature. The normalized emission spectra are identical and only show band-gap-related emission, but the nanowire layer shows a 20-fold higher emission intensity. This increased emission cannot be explained by the increase in absorptance alone, which only accounts for a factor of 1.4 (see the Supporting Information). Power-dependent PL emission

DOI: 10.1021/acs.nanolett.6b02971
Nano Lett. 2016, 16, 6467−6471

intensities are shown in Figure 2c (more information is given in the Methods section and the Supporting Information). The number of suns corresponding to the incident photon intensity is plotted on the top horizontal axis. From the absorbed and emitted photon intensities at 1 sun, we calculate $\eta_{ext} = (7.0 \pm 0.9) \times 10^{-4}$ for the nanowire array and $(5.2 \pm 0.5) \times 10^{-5}$ for the planar sample. The quasi-Fermi level splitting (equivalent to the maximum achievable V_{oc} in a contacted device) obtained from the integrated PL intensity is displayed on the right axis (full justification given in the Supporting Information). It is clear that nanostructuring increases the Fermi level splitting compared to the planar film for the entire excitation intensity range of 1 to 1000 suns. At 1 sun, the implied V_{oc} is 70 mV higher for the nanostructured sample compared to the planar sample, demonstrating that a nanostructured solar cell allows an intrinsic advantage in photovoltage over a planar layer.

The enhancement of the V_{oc} stems from a number of different contributions, as depicted schematically in Figure 1b. The first contribution is the reduction of material volume by a factor of 5.1, which therefore also reduces the nonradiative bulk recombination rate by the same factor as the nonradiative recombination rate is proportional to the number of bulk defect centers. If the total nonradiative recombination is dominated by bulk recombination (see the Supporting Information), this would result in an increase in V_{oc} of 42 mV. We emphasize that due to the optical antenna effect of the nanowires, the reduction in material volume does not decrease the short circuit current, as we will also discuss later. The second contribution to the improved V_{oc} is enhanced light outcoupling. We have simulated the photon escape probabilities (P_{esc}) for randomly oriented dipoles inside the absorption region of the material, shown in Figure 3, both for nanowire layers and for planar

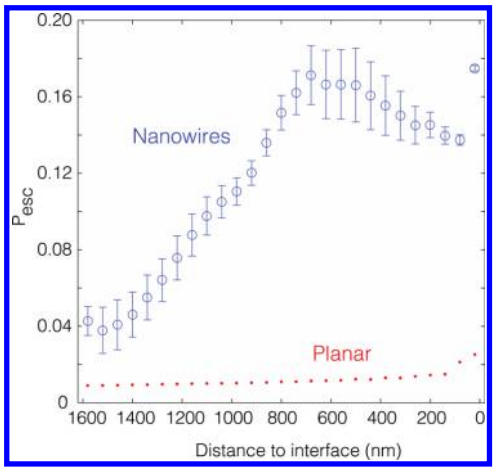

Figure 3. Photon escape probability for nanowires and planar samples. Simulated photon escape probability as a function of the distance to the nanowire layer−air or InP−air interface.

layers. We found average photon escape probabilities of 2.1% and 13% for the planar and nanowire samples, respectively (more details are given in section 5 of the Supporting Information), leading to an enhancement factor of 6.3. For materials with a low internal luminescence efficiency (<10%), this enhanced escape probability corresponds to an increase in V_{oc} of 47 mV. Because these effects together would result in a larger increase of V_{oc} (89 mV) than we have observed, we argue that increased surface recombination due to the increased surface area for the nanowires sample partially compensates the gain in V_{oc}. These results show, however, that even without additional surface passivation steps, the net V_{oc} is enhanced by nanostructuring. If we assume an average photon escape probability from the nanowire layer of 13%, we derive an $\eta_{int} \approx 0.54\%$ at 1 sun (comparison shown in the Supporting Information). We note that although a much-higher η_{int} has been reported for n-doped GaAs,[28] heavily n-doped InP[29] and InP micropillars,[27] we are not aware of such high η_{int} for the p-doped case.[30]

We emphasize that the V_{oc} enhancement is not a "concentration" effect because light concentration changes the entropy between the incident and emitted photons and thus modifies the thermodynamic limit given by V_{oc}^{rad}. To achieve a built-in concentration effect, one needs to modify the photon entropy. Such modification is, for example, achieved in concentrating photovoltaics, where an external lens modifies the angular distribution of incident light. Such a thermodynamic enhancement is in principle also possible using nanowire arrays, but this thus requires a specifically engineered angular emission profile.[31−33] We have checked the angular profiles of our nanostructured and planar samples, and they are not significantly different (Figure S6), so that we can exclude concentration due to photon entropy. Finally, the enhanced V_{oc} is not caused by effective band gap modification due to nanophotonic resonances[11] or different crystal structures, as we observe from the energy of the emitted PL. On the basis of these arguments, we can conclude that the V_{oc} enhancement can only be due to an effective volume reduction and an enhanced photon escape probability.

Finally, to explore the general effect of nanostructuring on the V_{oc}, we have used the more general form of eq 1, $V_{oc} = V_{oc}^{rad} - \frac{k_B T}{q}\left|\ln \frac{\eta_{int}\overline{P_{esc}}}{1-\eta_{int}(1-\overline{P_{esc}})}\right|$ (valid for any η_{int}, as long as there is no parasitic absorption), to investigate the potential for further improvement of present day solar cells by nanostructuring. In Figure 4a,b we have expressed the maximum V_{oc} (for InP) as a function of the photon escape probability and the material filling fraction f for two different values of η_{int}. The full equations are listed in the Supporting Information. We observe a clear logarithmic dependence of the maximum V_{oc} on $\overline{P_{esc}}$ and on f for the low internal luminescence efficiency. However, even layers with 90% internal luminescence efficiency can still gain tens of millivolts by improved photon escape probability and material volume reduction. Of course, the advantage vanishes when η_{int} approaches 1 very closely. Note that the choice of semiconductor defines only the value of the V_{oc} in the radiative limit and has no influence on the loss terms related to f and $\overline{P_{esc}}$, which makes these effects generic for all solar cell materials as long as surfaces are well-passivated. Figure 4 assumes that the surface recombination rate is small compared to the bulk recombination rate, while some materials instead suffer from high surface recombination velocities. However, for solar cell materials such as silicon[34,35] and GaAs,[36,37] it has already been shown that surface recombination can be greatly reduced by proper surface passivation. This is required to utilize nanostructured solar cells made of these materials.

For optimal solar cell performance, not only V_{oc} but also J_{sc} needs to be close to the theoretical maximum. As we have shown above, a reduction of material can substantially enhance light absorption, and we note that the volume can be reduced to at least a factor of $f \approx 0.08$ in (nano)wire arrays without losing any absorption with respect to a planar layer, as has been

DOI: 10.1021/acs.nanolett.6b02971
Nano Lett. 2016, 16, 6467−6471

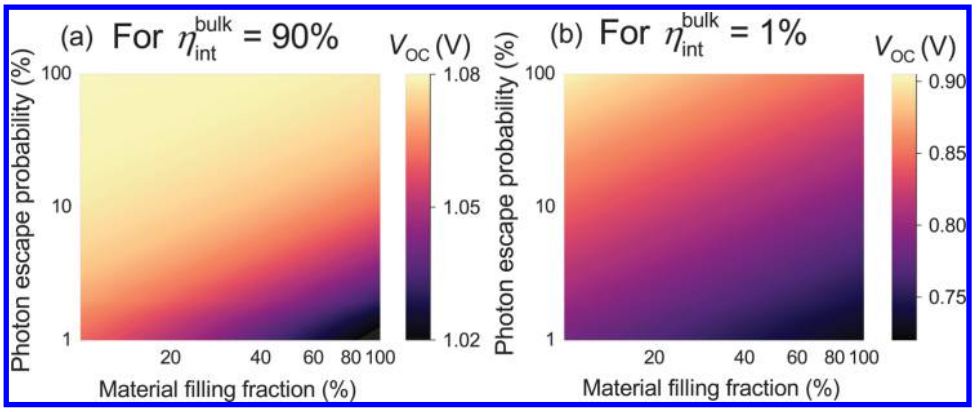

Figure 4. Enhancement of solar cell V_{oc} as a function of photon escape probability and material filling fraction. (a,b) Calculated V_{oc} values for InP cells expressed in a log–log plot as a function of the photon escape probability and the material filling fraction for a fixed internal radiative efficiency of 90% (a) and 1% (b).

demonstrated for materials such as silicon, InP, and GaAs.[19,38,39] This makes the relative increase in V_{oc} in Figure 4 also indicative of the relative increase in cell efficiency, although the exact improvement in efficiency depends on the exact geometry of the absorber. If the short-circuit current does not change, the relative efficiency improvement is comparable to the relative improvement in V_{oc}. From Figure 4, we can derive the optimum design requirements for new record high-V_{oc} solar cells: starting from a high internal radiative efficiency solar cell material, a very high photon escape probability should be combined with a very small amount of material. We finally conclude that nanostructuring is a very effective approach to increase both the solar cell photovoltage and the photocurrent to approach the Shockley–Queisser limit.

Methods. *Nanowire Array Fabrication.* The fabrication of our top-down etched nanowire array starts with MOVPE growth of an intrinsic InP layer on a Zn-doped InP (100) substrate at a temperature of 650 °C. An array of chromium nanodiscs is patterned by nanoimprint lithography. Subsequently, the Cr nanodisc pattern is transferred to an array of SiN_x nanocylinders by RIE etching. These SiN_x nanocylinders will serve as a hard mask for 40 min of ICP etching at 150 °C with CH_4 and H_2 etchant gases to form 1.6 μm high InP nanopillars. The nanowire surfaces are smoothed by digital sidewall etching (see the Supporting Information for SEM images). We use 10 etching cycles, each composed of a surface oxidation step and a chemical etching step, to selectively remove the oxide layer.

Photoluminescence Measurements. The samples were excited with a 532 nm continuous wave diode laser using a time-reversed Fourier microscope,[40] giving a plane wave on the sample with a spot radius of about 55 ± 5 μm. The photoluminescence was measured using an Andor Shamrock spectrograph equipped with an Andor iDus CCD camera. The collection efficiency of the setup at the emission wavelength was determined as is described in detail in the Supporting Information.

■ ASSOCIATED CONTENT

Supporting Information

The Supporting Information is available free of charge on the ACS Publications website at DOI: 10.1021/acs.nanolett.6b02971.

Additional details on external luminescence efficiency, fabrication of the etched nanowire array, the relation between the photoluminescence intensity and the quasi-Fermi level splitting, absorption in nanostructured and planar material, photon escape probabilities from nanowires and planar material, photoluminescence setup and calibration, comparison of internal radiative efficiency with VLS-grown InP nanowires, and calculation of the open circuit voltage. Figures showing V_{oc} as a function of the internal radiative efficiency and photon escape probability, SEM images of top-down etched InP NWs before and after digital sidewall etching, simulated absorption spectrum of nanowire array as used in the measurements, photon flux (rate per unit area) as used in the simulation, schematic overview of the time-reversed Fourier step, and unpolarized angle-dependent emission from nanowires and planar samples. (PDF)

■ AUTHOR INFORMATION

Corresponding Authors

*D.v.D. e-mail: a.d.v.dam@tue.nl.
*J.E.M.H. e-mail: j.e.m.haverkort@tue.nl.

Author Contributions

Y.C. and P.J.v.V. fabricated the etched nanowires. D.v.D. and N.J.J.v.H. performed the PL measurements. S.A.M. and D.v.D. did the numerical modeling. All authors participated in analyzing, discussing and interpreting the results. J.E.M.H., E.P.A.M.B., and E.C.G. supervised the research. D.v.D. wrote the manuscript with the valuable feedback of all authors. Y.C. and D.v.D. contributed equally to this paper.

Notes

The authors declare no competing financial interest.

■ ACKNOWLEDGMENTS

We acknowledge Jaime Gómez Rivas for the use of the time-reversed Fourier microscope setup of his group and Albert Polman for a careful reading of the manuscript. This work is supported by the Dutch Technology Foundation STW, which is part of the Netherlands Organization for Scientific Research (NWO), and is partially funded by the Dutch Ministry of Economic Affairs. It is also supported by the long-term energy and innovation program EOS-LT, funded by the Dutch national government. This work is also part of the research program of the Foundation for Research on Matter (FOM), which is part of the NWO.

DOI: 10.1021/acs.nanolett.6b02971
Nano Lett. 2016, 16, 6467–6471

REFERENCES

(1) Yablonovitch, E. *J. Opt. Soc. Am.* **1982**, *72*, 899.
(2) Campbell, P.; Green, M. A. *IEEE Trans. Electron Devices* **1986**, *33*, 234.
(3) Cao, L.; White, J. S.; Park, J.-S.; Schuller, J. A.; Clemens, B. M.; Brongersma, M. L. *Nat. Mater.* **2009**, *8*, 643.
(4) Polman, A.; Atwater, H. A. *Nat. Mater.* **2012**, *11*, 174.
(5) Brongersma, M. L.; Cui, Y.; Fan, S. *Nat. Mater.* **2014**, *13*, 451.
(6) Zhu, J.; Yu, Z.; Burkhard, G. F.; Hsu, C.-M.; Connor, S. T.; Xu, Y.; Wang, Q.; McGehee, M. D.; Fan, S.; Cui, Y. *Nano Lett.* **2009**, *9*, 279.
(7) Garnett, E. C.; Yang, P. *Nano Lett.* **2010**, *10*, 1082.
(8) Green, M. A.; Emery, K.; Hishikawa, Y.; Warta, W.; Dunlop, E. D. *Prog. Photovoltaics* **2015**, *23*, 805.
(9) Shockley, W.; Queisser, H. J. *J. Appl. Phys.* **1961**, *32*, 510.
(10) Sandhu, S.; Yu, Z.; Fan, S. *Opt. Express* **2013**, *21*, 1209.
(11) Sandhu, S.; Yu, Z.; Fan, S. *Nano Lett.* **2014**, *14*, 66.
(12) Kosten, E.D.; Atwater, J.H.; Parsons, J.; Polman, A.; Atwater, H.A. *Light Sci. Appl.* **2013**, *2*, e45 DOI: 10.1038/lsa.2013.1.
(13) Krogstrup, P.; Jørgensen, H. I.; Heiss, M.; Demichel, O.; Holm, J. V.; Aagesen, M.; Nygård, J.; Fontcuberta i Morral, A. *Nat. Photonics* **2013**, *7*, 306.
(14) Würfel, P. *Physics of Solar Cells*; Wiley-VCH Verlag: Weinheim, Germany, 2005.
(15) Miller, O. D.; Yablonovitch, E.; Kurtz, S. R. *IEEE J. Photovoltaics* **2012**, *2*, 303.
(16) Steiner, M. A.; Geisz, J. F.; Friedman, D. J.; Duda, A.; Olavarria, W. J.; Young, M.; Kuciauskas, D.; Kurtz, S. R.; Garcia, I. *IEEE J. Photovoltaics* **2013**, *3*, 1437.
(17) Ganapati, V.; Steiner, M. A.; Yablonovitch, E. *IEEE J. Photovoltaics* **2016**, *6*, 801.
(18) Rau, U.; Paetzold, U. W.; Kirchartz, T. *Phys. Rev. B: Condens. Matter Mater. Phys.* **2014**, *90*, 035211.
(19) Diedenhofen, S. L.; Janssen, O. T. A.; Grzela, G.; Bakkers, E. P. A. M.; Gómez Rivas, J. *ACS Nano* **2011**, *5*, 2316.
(20) Claudon, J.; Bleuse, J.; Malik, N. S.; Bazin, M.; Jaffrennou, P.; Gregersen, N.; Sauvan, C.; Lalanne, P.; Gérard, J.-M. *Nat. Photonics* **2010**, *4*, 174.
(21) Wallentin, J.; Anttu, N.; Asoli, D.; Huffman, M.; Åberg, I.; Magnusson, M. H.; Siefer, G.; Fuss-Kailuweit, P.; Dimroth, F.; Witzigmann, B.; Xu, H. Q.; Samuelson, L.; Deppert, K.; Borgström, M. T. *Science* **2013**, *339*, 1057.
(22) Joyce, H. J.; Wong-Leung, J.; Yong, C.-K.; Docherty, C. J.; Paiman, S.; Gao, Q.; Tan, H. H.; Jagadish, C.; Lloyd-Hughes, J.; Herz, L. M.; Johnston, M. B. *Nano Lett.* **2012**, *12*, 5325.
(23) Clapham, P. B.; Hutley, M. C. *Nature* **1973**, *244*, 281.
(24) Ross, R. T. *J. Chem. Phys.* **1967**, *46*, 4590.
(25) Würfel, P. *J. Phys. C: Solid State Phys.* **1982**, *15*, 3967.
(26) Rau, U. *Phys. Rev. B: Condens. Matter Mater. Phys.* **2007**, *76*, 1.
(27) Tran, T.-T. D.; Sun, H.; Ng, K. W.; Ren, F.; Li, K.; Lu, F.; Yablonovitch, E.; Chang-Hasnain, C. J. *Nano Lett.* **2014**, *14*, 3235.
(28) Schnitzer, I.; Yablonovitch, E.; Caneau, C.; Gmitter, T. J. *Appl. Phys. Lett.* **1993**, *62*, 131.
(29) Semyonov, O.; Subashiev, A.; Chen, Z.; Luryi, S. *J. Appl. Phys.* **2010**, *108*, 013101.
(30) Rosenwaks, Y.; Tsimberova, I.; Gero, H.; Molotskii, M. *Phys. Rev. B: Condens. Matter Mater. Phys.* **2003**, *68*, 115210.
(31) van Dam, D.; Abujetas, D. R.; Paniagua-Domínguez, R.; Sánchez-Gil, J. A.; Bakkers, E. P. A. M.; Haverkort, J. E. M.; Gómez Rivas, J. *Nano Lett.* **2015**, *15*, 4557.
(32) Xu, Y.; Gong, T.; Munday, J. N. *Sci. Rep.* **2015**, *5*, 13536.
(33) Anttu, N. *ACS Photonics* **2015**, *2*, 446.
(34) Oh, J.; Yuan, H.-C.; Branz, H. M. *Nat. Nanotechnol.* **2012**, *7*, 743.
(35) Repo, P.; Haarahiltunen, A.; Sainiemi, L.; Yli-Koski, M.; Talvitie, H.; Schubert, M. C.; Savin, H. *IEEE J. Photovoltaics* **2013**, *3*, 90.
(36) Joyce, H. J.; Parkinson, P.; Jiang, N.; Docherty, C. J.; Gao, Q.; Tan, H. H.; Jagadish, C.; Herz, L. M.; Johnston, M. B. *Nano Lett.* **2014**, *14*, 5989.
(37) Gao, Q.; Saxena, D.; Wang, F.; Fu, L.; Mokkapati, S.; Guo, Y.; Li, L.; Wong-Leung, J.; Caroff, P.; Tan, H. H.; Jagadish, C. *Nano Lett.* **2014**, *14*, 5206.
(38) Mariani, G.; Scofield, A. C.; Hung, C.-H.; Huffaker, D. L. *Nat. Commun.* **2013**, *4*, 1497.
(39) Kelzenberg, M. D.; Boettcher, S. W.; Petykiewicz, J. A.; Turner-Evans, D. B.; Putnam, M. C.; Warren, E. L.; Spurgeon, J. M.; Briggs, R. M.; Lewis, N. S.; Atwater, H. A. *Nat. Mater.* **2010**, *9*, 239.
(40) Grzela, G.; Paniagua-Domínguez, R.; Barten, T.; van Dam, D.; Sánchez-Gil, J. A.; Rivas, J. G. *Nano Lett.* **2014**, *14*, 3227.

DOI: 10.1021/acs.nanolett.6b02971
Nano Lett. 2016, 16, 6467−6471